

Variation of Turbulence Characteristics Along the Radius Under Different Gas Influx, ECRH Power and Plasma Currents in T-10 Tokamak

V.A. Vershkov, D.A. Shelukhin, S.V. Soldatov, S.A. Grashin, E.P. Gorbunov, Yu.V. Skosirev, V.F. Denisov, V.V. Chistiakov, T.B. Mialton, V.I. Pozniak, V.V. Piterskii, G.N. Ploskirev, V.M. Trukhin, D.V. Ryjakov, Yu.V. Gott, V.A. Krupin, N.N. Timchenko, M.V. Osipenko

Nuclear Fusion Institute, Russian Research Center "Kurchatov Institute"
123182, Kurchatov Sq. 1, Moscow, Russia

E-mail address of main author: vershkov@nfi.kiae.ru

Abstract: The turbulence characteristics were investigated by means of correlation reflectometry and Langmuir probes. The ECRH discharges show the distinct transition from the core turbulence, having complex structure, to the unstructured one at periphery. It is explained as the transition from ITG/TEM to the resistive interchange instability. The core turbulence includes the "broad band", "quasi-coherent" feature, arising due to the excitation of rational surfaces with high poloidal m-numbers, "low frequency", looking like "streamers" and oscillations at 20 – 30 kHz, having properties of "zonal flows". The turbulence rotates like rigid body with constant angular velocity equal to that of m=2 mode rotation over all plasma radii in OH discharges. The decrease of the mean core turbulence wavelength, impurities peaking and decrease of ion heat conductivity were observed under transition of the OH discharge from SOC to IOC phase after gas puff cut off. The change of poloidal asymmetry was also registered. Significant variation of the turbulence characteristics were measured at the start of the central ECRH and after fast edge cooling by carbon flake. In all cases the change of the core turbulence were interpreted as interplay between ITG and DTEM instabilities.

Three instabilities are considered as the cause of the core anomalous transport. These are Ion Temperature Gradient (ITG) [1], Dissipative Trapped Electron Mode (DTEM) [1] and Electron Temperature Gradient (ETG) [2]. The edge plasma turbulence may be caused by Drift Resistive Ballooning Mode instability DRB [3]. In such approach stability is determined by local plasma parameters and the fluctuations are excited by the temperature gradients, associated with the values of the heat fluxes, and stabilized by the steep density gradients. To study this approach, the turbulence characteristics were investigated over the whole plasma column in wide range of parameters from the most stable Ohmic discharge with peaked density up to the most unstable ECRH 1.4 MW discharges with flat density profiles. In difference to the local approach, a non-local plasma response to the fast perturbations was also observed in many experiments. With that aim the dynamic of turbulence evolution at the start of ECRH and fast edge cooling were investigated.

The T-10 heterodyne O-mode correlation reflectometer [4] and multipin movable Langmuir probe [5] were used to measure the properties of the small-scale plasma density fluctuations. Both diagnostics were able to measure poloidal turbulence characteristics. The reflectometer had the Low Field Side (LFS) and High Field Side (HFS) antennas.

Figure 1 presents the typical results of correlation analysis of reflectometry signals reflected from two poloidally separated points for the core and edge regions. Fourier spectra presented on the top traces, cross-phase between two signals on the middle and coherency on the bottom. A pronounce difference is clearly seen. The core turbulence rotates in electron diamagnetic drift direction (the slope of cross-phase trace) and has complex structure. It includes the background "Broad Band" (BB) fluctuation, High Frequency (HF) and Low Frequency (LF) "Quasi-Coherent" (QC) spectral maxima and "Low Frequency" (LF) peak near zero frequency. The experimental data evidenced that HF and LF QC arise due to the excitation of rational surfaces with high poloidal m-numbers [6]. They are similar to the "eddies", found in the 3D gyrokinetic simulations [7]. The LF have the features of the "streamers" [8] as they have long radial correlation length with zero phase shift [6]. A special

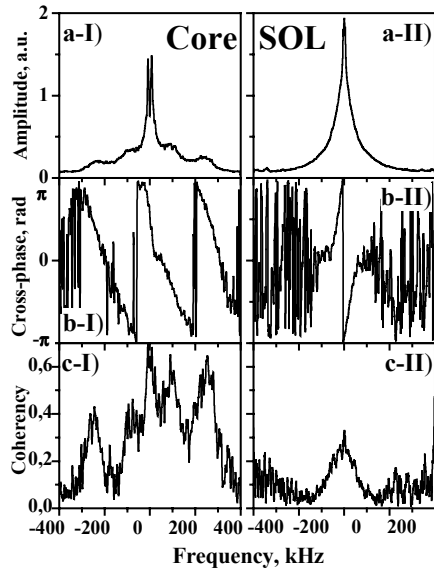


FIG. 1. Comparison of Fourier spectra of signals in plasma core fluctuations poloidal velocity, and in SOL region poloidal number and length.

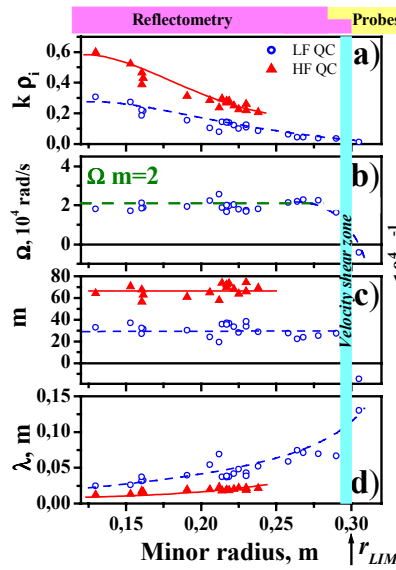


FIG. 2. The radial dependence of poloidal velocity, $\Omega m=2$, m , and $\lambda_z m$.

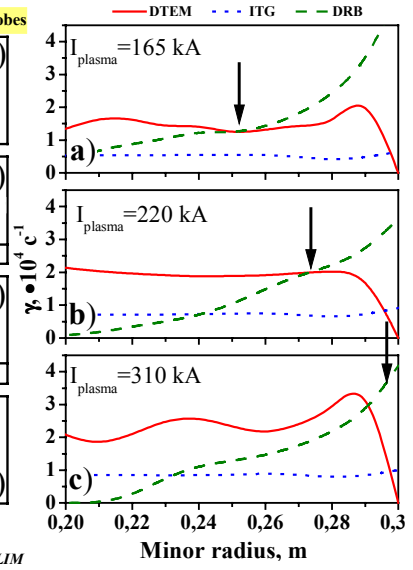


FIG. 3. Radial dependencies of ITG, DTEM and DRB instabilities growth rates

fluctuations at 20–30 kHz (not shown in Fig. 1) are seen at low densities near rational surfaces 2 and 3 [8, 5]. These oscillations are highly correlated at any poloidal separation of reflection points with zero phase shift. The probes data show that this feature is more pronounced in the potential fluctuation spectrum than in the density one. Their properties are very similar to the predicted by theory “zonal flows” [9]. In difference to the core turbulence, edge fluctuations have a smooth spectrum and rotate in the ion diamagnetic drift direction. Thus the turbulence velocity shear layer occurs at some radius. Probes measurements at the edge show that shear layer is determined by the reversal of the radial electric field [5]. The reversal of the turbulence rotation near the rail limiter in Ohmic discharge is shown in Fig. 2b. The reversal of the radial electric field in that case is naturally connected with the dramatic change of the electron-ion balance due to the parallel escape of the electrons to the limiter. In fact it was observed for Ohmic discharges in different conditions. The experimental radial positions of the velocity shear layer for ECRH discharges with plasma currents 165, 220 and 310 kA are shown in Fig. 3 with the arrows. It is clearly seen that the velocity shear layers are not connected with the limiter, but are shifted well inside the plasma. In this case the relative change of the electron-ion balance can be caused by the change of turbulence type from core ITG/TEM to the edge DRB. The calculated radial dependence of the growth rates for all three instabilities [1,3] are presented in Fig.3 by the different lines. One can see a good agreement of the experimental position of the shear layer with the regions where DRB become dominant. The validity of such approach is supported by the dependence of the shear layer position on the plasma current – it shifted deeper with the decrease of the current. So it can be concluded that in L mode the plasma edge is dominated by DRB, while core is connected with other instability types.

The typical core amplitude spectrum of fluctuations, shown in Fig. 1, exhibits two spectral maxima. The LF QC are usually observed at 50-100 and HF QC at 150-250 kHz. The bispectral analysis shows that these fluctuations are stochastically independent. The spectra evolution during SOC-IOC transition, shown in Fig. 4, proves that these are two different instabilities. The turbulence spectra measured at LFS (dashed line) and HFS (red line) for three time moments are presented. The reflection radii vary from 16 to 18 cm. A single maximum of LF QC turbulence was observed in SOC at frequency of 100 kHz only at LFS. As the transition to IOC phase was initiated via gas cut off, the density profile changes from the broad to the peaked one and the second maximum at 250 kHz appeared at both LFS and

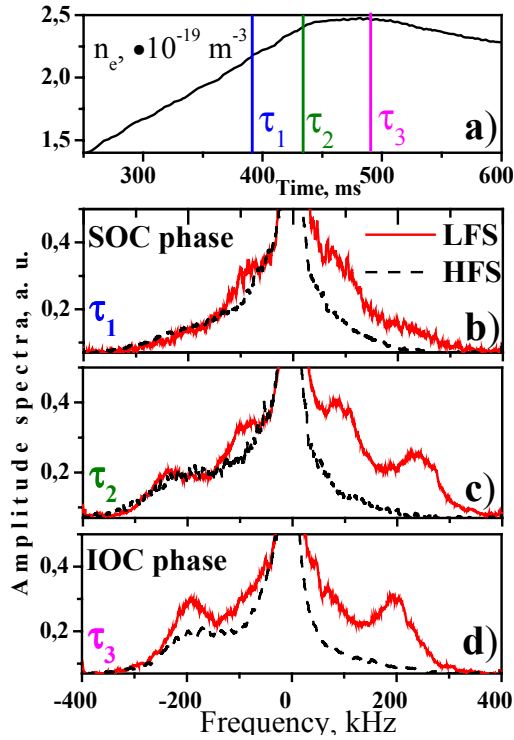
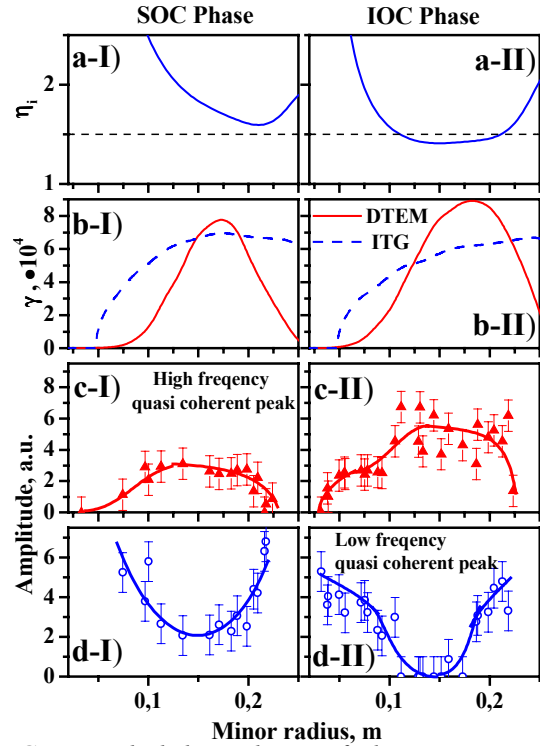


FIG. 4. Time evolution of the turbulence spectra on the LFS and HFS during transition from SOC and LF and HF QC characteristics in SOC and to IOC phase of the discharge



HFS. Finally only the oscillations at 200–250 kHz were seen in the spectra from LFS and HFS in IOC phase. So the physical difference of the LF and HF was verified by the difference in poloidal asymmetry. It should be underlined that the poloidal velocities were equal for both QC fluctuations. The spectrum evolution correlated with transition from anomalous ion heat conductivity, particles diffusion and pinch velocity, flat Zeff profile in SOC phase to the peaked Zeff and neoclassical ion heat conductivity in IOC phase. The radial dependence of $k_{\text{pol}} \cdot \rho_i$ value can be seen in Fig. 2a. This parameter approaches in the center to 0.3 for LF and 0.6 for HF QC. Early these maxima were interpreted as toroidal- and slab-ITG instabilities [10]. In present paper it is concluded that the LF oscillations looks like ITG instability, while the HF QC in IOC phase are similar to TEM turbulence. It should be mentioned that anomalous inward particles pinch was predicted for ion mixing instability [11] and plasma decontamination for impurity driven modes [12]. The detail analysis of the turbulence evolution over the whole radii during SOC to IOC transition after gas puff cut off may provide further insight in the physical origin of the core turbulence. Figure 5 presents the radial distributions of η_i , calculated growth rates of ITG and DTEM instabilities and amplitudes of HF and LF QC in SOC and IOC phases of discharge. It is clearly seen that in IOC phase LF is stabilized from 12 to 17.5 cm., while it exist near center and at periphery. At the same time HF is maximal at 15 cm. In difference in SOC phase LF is destabilized but HF significantly reduces. The stabilization of the LF is in good agreement with η_i decrease in IOC phase and occurs near its minimum. It is possible to conclude that LF and HF QC are similar to ITG and TEM instability, having nearly the same energy source. Thus the stabilization of one of them leads to increase of the other.

The analysis of the evolution of the turbulence characteristics in OH and ECRH discharges with different densities showed that the level of relative density fluctuation does not depend on density value with the exception of the cases of discharge shrinking just before the disruption. The turbulence level increases in a factor of 1.7 in ECR heating with the power about 1 MW with respect to the OH discharges. It is interesting that at low density the

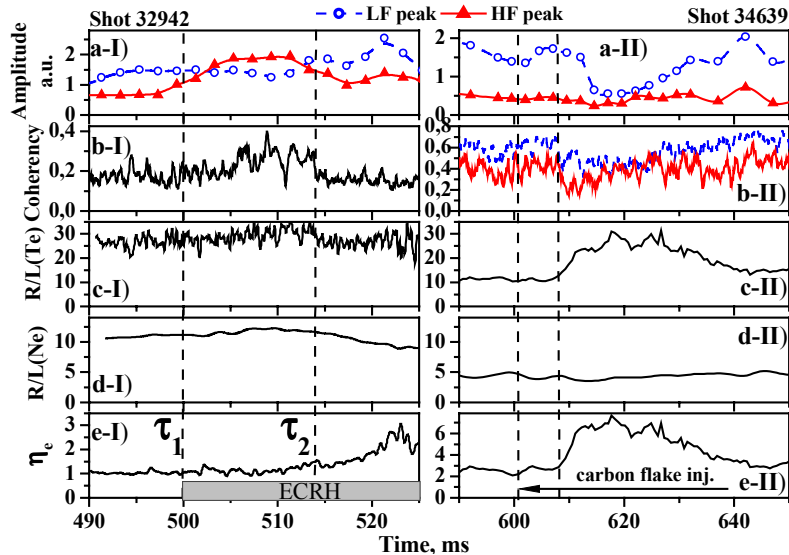


FIG. 6. Time traces of turbulence characteristics and plasma parameters after ECRH start and after carbon flake injection

plasma layers, which are radially far away of each other may be found in Fig. 2. It presents the radial dependence of turbulence parameters in the Ohmic discharge with current 300 kA, magnetic field 2.42 T and average density $4 \cdot 10^{19} \text{ m}^{-3}$. Figure 2b shows the radial variation of the angular turbulence rotation and Fig. 2c the poloidal m numbers of the LF and HF QC fluctuations. One can see that the angular turbulence rotation is remarkably constant over the whole plasma radii. Moreover it coincides with that of MHD $m/n=2/1$ island rotation. Figure 2c shows that the poloidal turbulence m numbers are also constant. Thus the turbulence rotates over all radii like rigid body with the angular velocity of $m=2$. It should be stressed that rigid body rotation together with the $m=2$ mode is the most general feature, seen practically in all OH discharges. It is clearly seen that this constraint breaks only at the velocity shear layer. Thus the experimental data makes possible to suggest that in some way the global interaction exist, which forced all fluctuations to rotate together with MHD $m=2$ island. Figure 2 shows that the constancy of poloidal m numbers (Fig. 2c) naturally leads to the short wavelength gyrobohm diffusion in the center with $k_{\text{pol}} \rho_i = 0.3$ and Bohm diffusion at the edge with $k_{\text{pol}} \rho_i = 0.05$.

The dynamic change of the turbulence was investigated in initial phase of central ECR heating, where the Ohmic confinement maintains up to 20 ms. after the heating start and deteriorates only after increase of edge recycling. This phenomenon of the Delay of Confinement Deterioration was earlier observed in ASDEX [13] with NBI and in T-10 [14] with ECRH. The turbulence properties evolution during initial phase of central ECRH are shown in Fig. 6-I. In spite of the decrease of the coherent properties of turbulence in stationary ECRH, significant increase of coherency was observed during first 5–20 ms. of the heating. The coherency increase disappeared shortly after the increase of plasma interaction with the wall and corresponding strong rise of recycling at the edge and broadening of the density profile. The HF QC fluctuations became dominant at the first 5–10 ms. They were gradually substituted by low frequency QC after beginning of density profile broadening. The expulsion of the high Z impurities under central ECRH was also observed in [6]. The excitation of TEM with subsequent transition to ITG after density profile broadening are consistent with theory. The reflection layer for the data in Fig. 6a was at 20 cm., but experiments with reflection layers from 6 to 20 cm gave the same result. At the ECRH start and in SOC/IOC transition high confinement occurs without the decrease of the turbulence amplitude, but with significant increase of coherent properties. This may be the consequence of the decrease of turbulence growth rate. So we may conclude that the increase of

turbulence frequency spectra in OH and ECRH are relatively narrow and dominated by LF QC, while at high density HF QC also appears. So it is possible to suggest that at low density ITG instability is important, but at higher densities both ITG and DTEM are present. Unfortunately now it is difficult to conclude which of the two instabilities make the biggest contribution to the plasma transport.

The evidences of some interaction between the

temperature gradients do not deteriorate transport provided that density remains peaked. The decrease of instability growth rate may be connected with the steeping of gradients due to Shafranov shift at higher plasma pressure. The time variation of the same set of turbulence characteristics after the strong edge cooling by carbon flake is presented in Fig. 6-II. The cooling occurs in discharge with current 180 kA and toroidal field 2.36 T. The sawtooth activity was stabilized due to peripheral ECRH heating with power about 0.3 MW. The strong electron temperature peaking at the reflection radius of 10 cm. is seen at 608 ms. It followed by the decrease of the coherency and strong reduction of LF QC. Thus the turbulence properties can be connected with the local plasma parameters. Both the ECRH and edge cooling leads to the peaking of temperature, but the change of coherency and QC amplitude is just opposite. Strong reduction of QC after flake injection can be explained by formation of the hollow impurity profile. In fact significant rise of Z_{eff} and SXR emission in the core are seen during the low QC amplitude phase. It can be supposed that redistribution of impurities plays an important role in the mechanism of LF QC turbulence as was pointed out in [12].

It is possible to conclude that experimental data in stationary conditions and in dynamics can be well described with the local turbulence model, including ITG/TEM in the core and DRB at the edge. The experimental data shows that the high confinement discharges exhibit strong QC spectral peaks, while for the low confinement cases small contrast of the QC fluctuations is typical. The decrease of the QC at low confinement may occurs because the turbulence become more stochastic with the increase of the turbulence growth rate. So the excitation of the helical modes with high m numbers decreases. The phenomenon of rigid body turbulence rotation together with MHD $m=2$ mode implies some mechanisms of interaction of short wave turbulence with the global MHD modes at all plasma radii. The dynamic behavior of the turbulence in initial phase of the ECRH contradict to the critical temperature gradient model because the increase of the temperature gradients do not lead to the transport deterioration, but even increase turbulence coherent properties. Edge cooling shows possible influence of impurity distribution on turbulence properties.

This work is supported by Nuclear Science and technology Department of Minatom RF and Grants: RFBR (00-15-96536), INTAS (2001-2056) and NWO RFBR (047.009.009).

References

- [1] J. Weiland, H. Nordman, Nuclear Fusion, **31**, (1991), 390.
- [2] B.B. Kadomtsev, O.P. Pogutse, Rev. Plasma Phys., Vol. 5, Chapter 2.
- [3] M.V. Osipenko *et al* Physika Plasmy V. 26, N. 12, (2000), 1.
- [4] V.A. Vershkov *et al* RSI, V. 70, N. 3, (1999), 2903.
- [5] V.A. Vershkov *et al*, Proc. 28 EPS Conf. Plasma Phys. Contr. Fusion, Funchal, V. 25A, (2001), 1273.
- [6] V.A. Vershkov *et al* Proc. 26 EPS Conf. Plasma Phys. Contr. Fusion, Maastricht, V. 23J, (1999), 825.
- [7] R.E. Waltz *et al* Phys. Plasmas **1**, (1994), 2229.
- [8] V.A. Vershkov *et al*, Proc. 28 EPS Conf. Plasma Phys. Contr. Fusion, Funchal, V. 25A, (2001), 1413.
- [9] G. Manfredi *et al*, Plasma Phys. Contr. Fusion, **43**, (2001), 825.
- [10] V.A. Vershkov *et al*, Nuclear Fusion (Yokohama Special Issue 2), **39**, (1999), 1775.
- [11] B. Coppi, C. Slight, Phys. Rev. Lett., **14**, (1978), 551.
- [12] B. Coppi, G. Rewoldt, T. Schep, Phys. Fluids, **19**, (1976), 1144.
- [13] G. Fussman *et al* Proc. 12 IAEA Conf. Plasma Phys. and Contr. Fus., Nice, V. 1, IAEA, Vienna, (1989), 145.
- [14] A. V. Sushkov *et al*, Proc. 17 EPS Conf. Plasma Phys. Contr. Fusion, Amsterdam, V. 14B, Part III, (1990), 1076.

